Ellipsometry in a Uniaxial ZnO Thin Film

Author: Alejandro Gil Morente, agilmore32@alumnes.ub.edu
Facultat de Física, Universitat de Barcelona, Diagonal 645, 08028 Barcelona, Spain.

Advisor: Jordi Gomis i Bresco, jordi.gomis.bresco@ub.edu

Abstract: In this work, the indexes of refraction of a uniaxial anisotropic, inhomogeneous thin film of ZnO grown on a glass substrate are determined in the transparent region using spectroscopic four-modulator generalized ellipsometry (4-MGE). Three different points of the sample are studied at three angles of incidence and the real and imaginary parts of the coefficient $\rho = t_{pp}/t_{ss}$ are obtained and fitted from 450 to 800 nm assuming zero absorption. The results lead to very accurate values of the parameters used for the model, which include the thickness of the film and the resonant wavelengths with nanometer precision. The obtained functions are then compared to the tabulated data of the bulk material, showing a clear reduction of the refractive indexes of roughly 0.15 in the whole range. The effects of the inhomogeneity of the sample are reflected in the dispersion of the obtained refractive index values from point to point.

Keywords: zinc oxide, thin film, anisotropy, ellipsometry, refractive index.
SDGs: 3 (Good Health and Well-Being), 7 (Affordable and Clean Energy), 9 (Industry, Innovation and Infrastructure)

I. INTRODUCTION

Zinc oxide is a semiconductor that can crystallize in a wurtzite structure, which induces uniaxial anisotropy. This results in a single principal axis of symmetry defined as the optic axis (OA) of the crystal. Unlike isotropic materials, the electric field of light will be altered differently depending on its polarization direction within the crystal and how the optic axis is oriented.

Optical properties can be described by the complex, wavelength dependent refractive index

$$\tilde{n}(\lambda) = n(\lambda) + ik(\lambda)\,, \qquad (1)$$

where n is the refractive index related to the phase velocity of light, k is the extinction coefficient related to the absorption of light, and λ is the wavelength of light. In a uniaxial crystal, n is referred to as ordinary (n_o) for light polarized perpendicular to the OA, and extraordinary (n_e) for light polarized parallel to the OA.

Due to the large bandgap of this material (~3.3 eV), both electrical and optical properties of ZnO are at the center of attention of the scientific community. Its transparent region coincides with the visible light spectrum, which, when doped, makes it a special type of material known as Transparent Conductive Oxide.

When light reaches a surface, it is either transmitted or reflected. Considering a thin film whose thickness is comparable to the coherence length of incident light, the incoming ray will transmit through the film and will experience multiple internal reflections between the top and bottom surfaces, exiting the material at each of them while losing intensity, as k is non-zero and absorption exists at a very low rate in the film. The resulting reflected and transmitted beams will be the sum of the multiple transmitted rays at the top and bottom of the thin film respectively, due to the successive internal reflections (Fig. 1).

The ratio of light polarized parallel (p) and perpendicular (s) to the plane of incidence (POI) between the transmitted and incident rays in an interface is given by the Fresnel coefficients t_{pp} and t_{ss} respectively, which depend on the angle of incidence (AOI). Since light properties in the film are defined by the complex index $\tilde{n}$, t_{pp} and t_{ss} are also complex quantities. When the sample is anisotropic, other terms can be considered to study the change from s- to p-light (t_{sp}) and vice versa (t_{ps}), also known as cross-polarization coefficients.

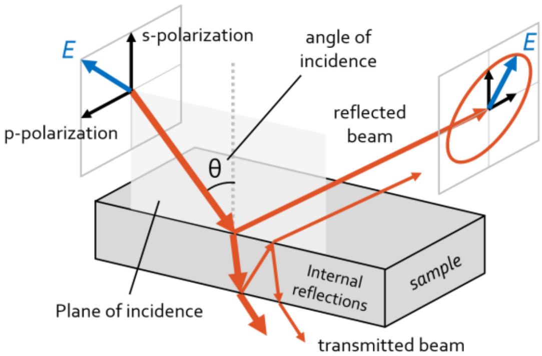

Fig. 1. Interaction of linearly polarized light at 45° when reaching a thin film. The beam may be both reflected and transmitted through the sample, experiencing multiple internal reflections and a change in its polarization state after the process.

One of the techniques that has gained popularity in recent years to study how light is altered by an optical element such as an anisotropic thin film and characterize it is Mueller matrix spectroscopic ellipsometry (MMSE). A

Mueller matrix (MM) is a real-valued 4x4 matrix that describes an optical system that modifies the polarization of light and connects the input and output states of light before entering and after exiting the sample [1]:

$$\boldsymbol{S_{out}} = \boldsymbol{MS_{in}}\,. \tag{2}$$

Here S are real-valued 4x1 Stokes vectors describing the state of light at these given points with six intensity measurements for different polarizations:

$$\boldsymbol{S} = \begin{bmatrix} S_0 \\ S_1 \\ S_2 \\ S_3 \end{bmatrix} = \begin{bmatrix} I_x + I_y \\ I_x - I_y \\ I_{+45°} - I_{-45°} \\ I_R - I_L \end{bmatrix}, \tag{3}$$

where I_x, I_y, $I_{+45°}$ and $I_{-45°}$ are the intensities of linearly polarized light oriented along the x, y, +45°, and -45° directions, respectively, and I_R and I_L are the intensities of right and left circular polarizations, respectively. In the case of MMSE, x and y orientations match the p and s polarization directions for the sample.

The Mueller matrix $\boldsymbol{M}$ describes the properties of the sample regardless of the type of incoming light and only for a specific measurement (reflection or transmission) and angle of incidence. Both Stokes vectors and Mueller matrices are often normalized to the total intensity when it is irrelevant for the experiment, so that information about polarization changes becomes independent of absolute intensity. The normalized Mueller matrix is given by

$$\boldsymbol{M} = \begin{bmatrix} 1 & m_{01} & m_{02} & m_{03} \\ m_{10} & m_{11} & m_{12} & m_{13} \\ m_{20} & m_{21} & m_{22} & m_{23} \\ m_{30} & m_{31} & m_{32} & m_{33} \end{bmatrix}, \tag{4}$$

where $m_{ij} = M_{ij}/M_{11}$ are the normalized MM elements constrained between -1 and $+1$, and M_{11} describes the transmitted intensity for unpolarized light. Each MM element indicates how a certain light polarization will be converted to another from the ones described by $\boldsymbol{S}$ due to the properties of the sample. When an element converts an incoming polarization into its opposite counterpart, it becomes negative. The MM for an anisotropic material can be rewritten in the NCS representation as [2]

$$\boldsymbol{M}_a = \begin{bmatrix} 1 & -N - \alpha_{ps} & C_{sp} + \zeta_1 & S_{sp} + \zeta_2 \\ -N - \alpha_{sp} & 1 - \alpha_{sp} - \alpha_{ps} & -C_{sp} + \zeta_1 & -S_{sp} + \zeta_2 \\ C_{ps} + \xi_1 & -C_{ps} + \xi_1 & C + \beta_1 & S + \beta_2 \\ -S_{ps} + \xi_2 & S_{ps} + \xi_2 & -S + \beta_2 & C - \beta_1 \end{bmatrix}. \tag{5}$$

Here N, C and S are three ellipsometry parameters that directly relate to the complex ratio

$$\rho = \frac{t_{pp}}{t_{ss}} = \frac{C + iS}{1 + N}\,. \tag{6}$$

A good determination of ρ is crucial for the complete characterization of the sample, since it condenses all the information about polarization changes within the thin film and, subsequently, about its optical functions and crystalline structure. If the crystal optical functions are well-known, the thickness can also be determined from the MMSE data.

When measuring anisotropic materials, the MM will depend on the orientation of the OA relative to the plane of incidence. If the symmetry axes of the sample are perfectly aligned parallel or perpendicular to the POI, the 2x2 top-right and bottom-left sections of the MM related to cross-polarization will vanish, and the matrix will take the form of an isotropic sample, with only 8 elements. In this configuration, the cross-polarization coefficients t_{sp} and t_{ps} are zero and the analysis is reduced to t_{pp} and t_{ss} [3].

Many types of ellipsometers can measure different regions of the MM depending on the set of optical elements that they include. The instrument used for this work is a spectroscopic 4-modulator generalized ellipsometer (4-MGE) in transmission mode, which is able to measure the 16 from the MM at once and is displayed in Fig. 2.

The 4-MGE uses a Xe lamp as a source of unpolarized light (1), four photoelastic modulators (PEM), from which two of them are located in the polarization state generator (PSG) (2) before the sample (3) and the other two in the polarization state analyzer (PSA) (4) after the sample, a linear polarizer right before the PSG and another (analyzer) after the PSA, a monochromator and a detector (5), and a data acquisition system. The PSG and PSA introduce periodic modulation of the polarization of light in multiple states and operate at different frequencies to allow a unique codification of the MM elements in the detected signal.

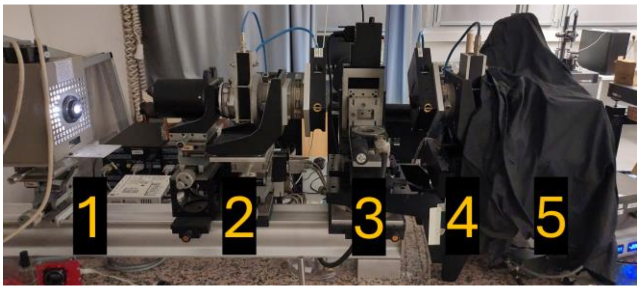

Fig. 2: Picture of the 4-MGE used at the laboratory with the different elements indicated with numbers, in order: Xe lamp, PSG, sample, PSA, monochromator and detector (not visible).

In this manner, light is emitted from the Xe lamp and enters the PSG, where it is first modulated in different polarization states, including linear, elliptic, and circular. Then light is transmitted through the anisotropic sample and reaches the PSA being already altered. The PSA analyzes the emerging light and decomposes it in multiple polarization states to capture the complete information on how it was modified by the sample. Finally, the monochromator filters the light at each wavelength from a selected range, and the detector measures the intensity in order to send it to the computer and analyze the detected signal with a Fourier transform. The final data is the 16 elements of the MM as functions of wavelength.

II. EXPERIMENTAL SETUP

A thin film of ZnO was previously grown on a glass substrate with its OA perpendicular to the surface plane, using RF magnetron sputtering. Due to the quality of the instrument, the sample was expected to have a non-uniform thickness. For the in-situ preparation, the surface of the sample was cleaned with isopropyl alcohol and a lens paper.

In order to set the first calibration, the MM was only measured with air, to check that the elements of the diagonal m_{11}, m_{22}, m_{33} were the closest to 1 and any other m_{ij} was 0. Then, the angular reference was defined in normal incidence. Finally, the sample was placed and rotated until m22 and m33 were the closest to 1, to have the ZnO thin film properly oriented with respect to the plane of incidence and fix the rotation axis for every AOI.

The 4-MGE measurements were made on the sample oriented with the OA parallel to the POI. Three angles of incidence were used (40°, 50° and 60°) and wavelength covered the range from 350 to 800 nm, including the visible spectrum and a small portion of the UV.

The optical resolution of the system is ~1 nm. The step size was set at 2 nm. Three different points of the surface were analyzed by following a vertical line from the bottom to the top of the square near the edges, with approximately the same distance between them.

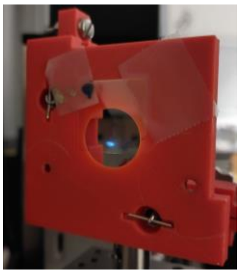

FIG. 3. Picture of the experimental assembly in the laboratory where the sample is being illuminated at the bottom point.

III. RESULTS AND DISCUSSION

As expected from the chosen, particular orientation of the thin film, the cross-polarization terms (m_{02}, m_{03}, m_{12}, m_{13}, m_{20}, m_{21}, m_{30}, m_{31}) become negligible, since they are 3 orders of magnitude smaller compared to the other 8 elements from the MM. These terms might have appeared due to a minimal tilt of the OA outside the POI during the setup. Nevertheless, they were considered 0 within the experimental error, confirming that cross-polarization vanishes in this configuration. Thus, the matrix is reduced to 8 elements.

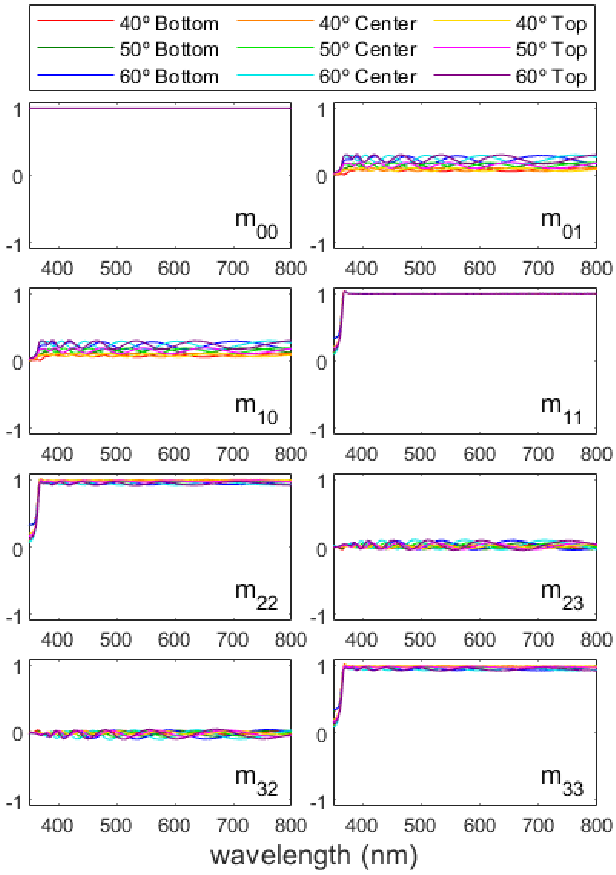

FIG. 4. Normalized Mueller matrix coefficients for 40º, 50º and 60º oblique angles of incidence at three different points of the ZnO sample for the measured wavelength range (350-800 nm).

As can be seen from Fig. 4, elements show small oscillations due to constructive and destructive interferences inside the film, which increase in amplitude with AOI. Element m_{11} remains close to 1 and practically constant from ~380 nm, indicating low depolarization. m_{22} and m_{33} behave similarly, although they seem more sensitive to thin film interferences. At short wavelengths (350-380 nm), major deviations are present and may be linked to complex interactions related to absorption near the band edge, where k should not be dismissed. Due to this abrupt behavior at shorter wavelengths, n was later fitted from 450 nm to assure a fully transparent region where oscillations are stabilized, with k set to 0.

It is worth noting that the AOI slightly alters the area of the light beam on the sample, increasing as the angle becomes larger, while the point of incidence stays fixed. Given the significant inhomogeneity of our sample, this change in area had an impact on the accuracy of the measurements.

The NCS parameters were extracted from Eq. 5 as

$$\begin{bmatrix} N \\ C \\ S \end{bmatrix} = \frac{1}{2}\begin{bmatrix} 1 - m_{11} - m_{01} - m_{10} \\ m_{22} + m_{33} \\ m_{23} - m_{32} \end{bmatrix} \quad (7)$$

in order to determine the real and imaginary parts of ρ (see Eq. 6). At this point, 6 functions were obtained for each measured point on the sample, as three different angles of incidence were used.

In the transparent region below the band edge, the real part of the refractive indices is frequently well represented by the Sellmeier approximation

$$n(\lambda) = \sqrt{1 + A\frac{\lambda^2}{\lambda^2 - \lambda_0^2}}, \quad (8)$$

where n(λ) is the refractive index as a function of wavelength, A is the amplitude and λ_0 is the resonant wavelength.

The experimental values of $Re(\rho)$ and $Im(\rho)$ at the three measured AOIs, depicted in Fig. 5, were simultaneously fit for each point in the wavelength region 450-800 nm (within the transparent region) to two Sellmeier approximations for the ordinary and extraordinary refractive indexes, with $k = 0$. For this purpose, the mathematical model developed in MATLAB by Nichols [4] was used and a simple program was built on the previous one to meet our requirements. This simplified model involved five different parameters (thickness d, A_o, $\lambda_{0,o}$, A_e, and $\lambda_{o,e}$) that were determined by introducing approximated, well-known values and finding a local minimum of a non-linear regression afterwards.

TABLE I. Sellmeier fits to the real and imaginary parts of ρ for the three studied AOIs at each point of the sample. The wavelength range was 450-800 nm.

	Point 1 "Bottom"	Point 2 "Center"	Point 3 "Top"
d (nm)	765.9 ± 1.1	825.7 ± 0.9	869.1 ± 0.9
A_o	2.117 ± 0.007	2.170 ± 0.006	2.190 ± 0.006
$\lambda_{0,o}$ (nm)	212.0 ± 1.2	209.1 ± 0.8	211.4 ± 0.7
A_e	2.172 ± 0.008	2.231 ± 0.006	2.234 ± 0.006
$\lambda_{0,e}$ (nm)	206.7 ± 1.3	205.5 ± 0.9	208.6 ± 0.8

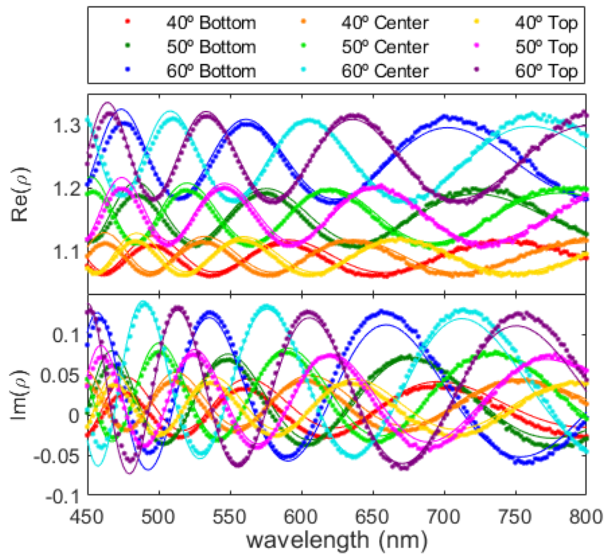

FIG. 5. Real and imaginary parts of ρ at 40º, 50º and 60º oblique angles of incidence at three different points of the ZnO thin film with its OA oriented parallel with respect to the plane of incidence. The wavelength range is 450-800 nm.

The parameters obtained are shown in Table I. The small errors indicate that the fits are good. The thickness of the sample varies between 765 and 870 nm, evidencing the inhomogeneity of the film. The functions of ρ were simulated with these parameters and included in Fig. 5 with solid lines, showing only minimal deviation from the experimental values at shorter wavelengths near the absorption region, since this model does not consider k. Even so, functions from every point are well matched.

As can be observed in Fig. 5, both real and imaginary parts of ρ amplify their oscillations with greater angles, as it was commented on Fig 4. As the AOI increases, anisotropy effects are more pronounced and the effective optical path within the film changes more drastically with λ, resulting in both an increase and major fluctuation of ρ. $Re(\rho)$ always stays over 1 ($|t_{pp}| > |t_{ss}|$), proving that the thin film transmits p-polarization more efficiently than s-polarization.

The measurements at the three positions (bottom, center, top) show consistent trends for both $Re(\rho)$ and $Im(\rho)$, indicating that the ZnO thin film is relatively uniform across the sample in terms of roughness. Furthermore, the lack of significant damping and/or distortion in the fluctuations of these functions confirm a negligible absorption, resulting in a refractive index primarily dictated by dispersion in the whole range.

Another model was also tested considering the ZnO thin film as isotropic, where $n_o = n_e$, yet the results deviated abnormally from the experimental values. Great AOIs are considered in this study, for which the anisotropic effects strengthen. For this reason, an isotropic nature of the sample was discarded.

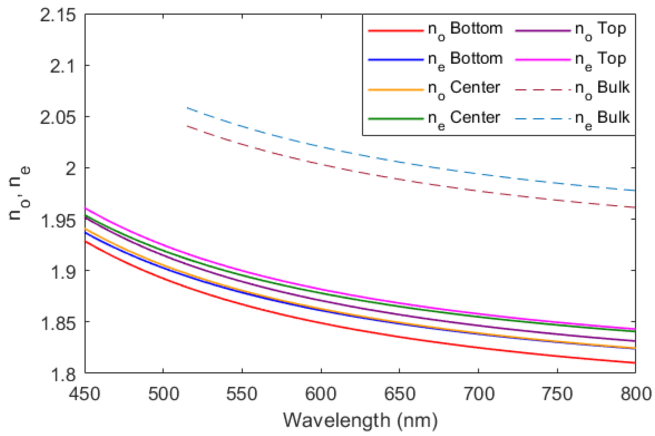

FIG. 6. Ordinary and extraordinary indexes of refraction of the sample, determined at three points of different thicknesses with the parameters from Table I. Data from [5] is included for a comparison between thin film and bulk state.

The two Sellmeier fits of n_o and n_e obtained for each point of the sample are shown in Fig. 6 and compared to the 2-MGE data obtained by Jellison in [5] for an anisotropic crystal bulk of ZnO with its OA parallel to the POI. With regard to the parameters from the fit, the amplitudes A_o, A_e found in this work differ from the bibliography on average by 0.5 below. As for the resonant wavelengths, the maximum deviation is only 6 nm above Jellison's.

As can be seen in Fig. 6, every ordinary refractive index is lower than its correspondent extraordinary index, consistent with the uniaxial anisotropic nature of our grown sample. The optical functions decrease smoothly with λ, very similarly to the bulk material, with a difference of ~ 0.15 below and practically constant over the whole range, that equals a drop of roughly 7% from bulk behavior in the transparent region. This difference could be attributed to a less dense crystalline structure in a thin film, as well as to surface effects.

It is also worth to highlight the spatial variation of n depending on the position (bottom, center, top) due to the inhomogeneity of the film. For this reason, the birefringence $\Delta n = n_e - n_o$ has not been studied since dispersion is very high, which would lead to ambiguity in the results.

IV. CONCLUSIONS

- The spectroscopic four-modulator generalized ellipsometer from the laboratory has been proven to be highly precise in the determination of the thickness of our ZnO thin film at different points of the sample, with an estimated error of 1 nm.
- A mathematical model has been used and edited for fitting the real and imaginary parts of the ratio ρ in the transparent region of the material successfully. The results are promising, even though the extinction coefficient has not been considered. Thus, this work has shown a potential alternative in characterizing anisotropic thin film samples grown with RF magnetron sputtering by directly calculating a single ellipsometry parameter.
- The ordinary and extraordinary indexes of refraction found have demonstrated the uniaxial anisotropic structure of the ZnO sample. Measuring at different angles of incidence has been essential to unveil this nature due to the increasing oscillations of ρ observed at greater angles, as well as for obtaining more accurate optical parameters. When compared to the bibliography, a remarkably similar pattern has been observed at lower values, with a very slight variation in resonant wavelengths between the thin film and the crystal bulk forms.

Acknowledgments

I would like to thank Jordi Gomis, who has been an excellent advisor and has treated me with kindness and proximity during the whole work, even in hard times. He has strengthened my will to continue studying light applications. I also want to thank especially my mother and my best friend from university, for being very supportive and always encouraging me to give my best.

[1] J. N. Hilfiker, N. Hong, and S. Schoeche, "Mueller matrix spectroscopic ellipsometry," *Advanced Optical Technologies*, vol. 11, no. 3–4, pp. 59–91, Jun. 2022.

[2] H. G. Tompkins and E. A. Irene, *Handbook of Ellipsometry*. 2005.

[3] G. E. Jellison, N. J. Podraza, and A. Shan, "Ellipsometry: dielectric functions of anisotropic crystals and symmetry," *Journal of the Optical Society of America A*, vol. 39, no. 12, p. 2225, Oct. 2022.

[4] S. Nichols, "Coherence in Polarimetry," PhD dissertation, New York University, 2018.

[5] G. E. Jellison, "Optical functions of uniaxial zinc oxide (ZnO) revisited," *Surface Science Spectra*, vol. 30, no. 2, Aug. 2023.

El·lipsometria en una Capa Prima Uniaxial de ZnO

Author: Alejandro Gil Morente, agilmore32@alumnes.ub.edu
Facultat de Física, Universitat de Barcelona, Diagonal 645, 08028 Barcelona, Spain.

Advisor: Jordi Gomis i Bresco, jordi.gomis.bresco@ub.edu

Resum: En aquest treball, els índexs de refracció d'una capa prima anisotròpica uniaxial i no homogènia de ZnO crescuda sobre un substrat de vidre es determinen a la regió transparent mitjançant el·lipsometria generalitzada espectroscòpica de quatre moduladors (4-MGE). S'estudien tres punts diferents de la mostra en tres angles d'incidència, i les parts real i imaginària del coeficient $\rho = t_{pp}/t_{ss}$ s'obtenen i s'ajusten de 450 a 800 nm assumint una absorció nul·la. Els resultats condueixen a valors molt precisos dels paràmetres utilitzats per al model, que inclouen el gruix de la pel·lícula i les longituds d'ona de ressonància amb precisió nanomètrica. Després, les funcions obtingudes es comparen amb les dades tabulades del material en forma "bulk", mostrant una clara reducció dels índexs de refracció d'aproximadament 0.15 en tot el rang. Els efectes de la inhomogeneïtat de la mostra es reflecteixen en la dispersió de punt a punt dels valors de l'índex de refracció obtinguts.

Paraules clau: òxid de zinc, capa prima, anisotropia, el·lipsometria, índex de refracció.

ODSs: Aquest TFG està relacionat amb els següents Objectius de Desenvolupament Sostenible (SDGs):

Objectius de Desenvolupament Sostenible (ODSs o SDGs)

1. Fi de la es desigualtats		10. Reducció de les desigualtats	
2. Fam zero		11. Ciutats i comunitats sostenibles	
3. Salut i benestar	X	12. Consum i producció responsables	
4. Educació de qualitat		13. Acció climàtica	
5. Igualtat de gènere		14. Vida submarina	
6. Aigua neta i sanejament		15. Vida terrestre	
7. Energia neta i sostenible	X	16. Pau, justícia i institucions sòlides	
8. Treball digne i creixement econòmic		17. Aliança pels objectius	
9. Indústria, innovació, infraestructures	X		

El contingut d'aquest TFG del grau universitari de Física es relaciona amb l'ODS 7, ja que el material estudiat pot afavorir un increment en l'obtenció d'energia solar en cel·les solars, i amb l'ODS 9, perquè la tècnica utilitzada permet la caracterització de capes primes que poden formar part d'una producció a nivell industrial i el material tractat es pot combinar amb altres en sistemes multicapa per tal de desenvolupar noves tecnologies. També es pot relacionar amb l'ODS 3, ja que el·lipsometria permet estudiar i delimitar teixits cancerosos o en mal estat degut al canvi en la resposta a la llum polaritzada.